Applied Energy 285 (2021) 116470

Contents lists available at ScienceDirect

Applied Energy

journal homepage: www.elsevier.com/locate/apenergy

Medium-temperature thermochemical energy storage with transition metal ammoniates – A systematic material comparison

Danny Müller [a,*], Christian Knoll [a,b], Georg Gravogl [a,g], Christian Jordan [b], Elisabeth Eitenberger [c], Gernot Friedbacher [c], Werner Artner [d], Jan M. Welch [e], Andreas Werner [f], Michael Harasek [b], Ronald Miletich [g], Peter Weinberger [a,*]

[a] Institute of Applied Synthetic Chemistry, TU Wien, Getreidemarkt 9, 1060 Vienna, Austria
[b] Institute of Chemical, Environmental and Bioscience Engineering, TU Wien, Getreidemarkt 9, 1060 Vienna, Austria
[c] Institute of Chemical Technologies and Analytics, TU Wien, Getreidemarkt 9, 1060 Vienna, Austria
[d] X-Ray Center, TU Wien, Getreidemarkt 9, 1060 Vienna, Austria
[e] Center for Labelling and Isotope Production, TRIGA Center Atominstitut, TU Wien, Stadionallee 2, 1020 Vienna, Austria
[f] Institute for Energy Systems and Thermodynamics, TU Wien, Getreidemarkt 9, 1060 Vienna, Austria
[g] Institut für Mineralogie und Kristallographie, University of Vienna, Althanstraße 14, 1090 Vienna, Austria

HIGHLIGHTS

- Transition metal salts react reversibly and highly exothermic with ammonia.
- Highest storage densities are 8.75 GJ m^{-3} for $NiCl_2$ and 6.38 GJ m^{-3} for $CuSO_4$.
- Ammonia uptake and release is fully reversible.
- Transition metal sulphates feature perfect cycle stability.
- Operational temperature window for energy storage ranges between 25 and 350 °C.

GRAPHICAL ABSTRACT

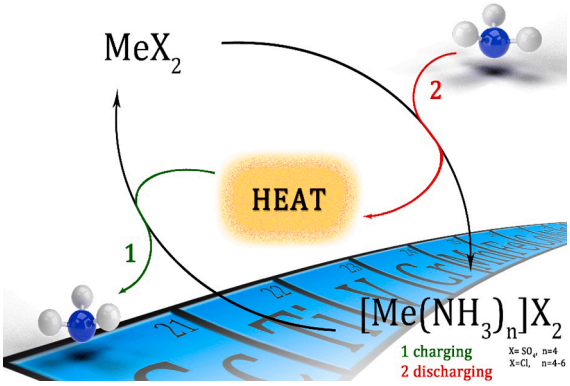

ARTICLE INFO

Keywords:
Ammonia
Transition metal salts
Transition metal ammoniates
Thermochemical energy storage materials
Thermochemistry

ABSTRACT

Materials with high volumetric energy storage capacities are targeted for high-performance thermochemical energy storage systems. The reaction of transition metal salts with ammonia, forming reversibly the corresponding ammonia-coordination compounds, is still an under-investigated area for energy storage purposes, although, from a theoretical perspective this should be a good fit for application in medium-temperature storage solutions between 25 °C and 350 °C.

In the present study, the potential of reversible ammoniation of a series of transition metal chlorides and sulphates with gaseous ammonia for suitability as thermochemical energy storage system was investigated. Among the investigated metal chlorides and sulphates, candidates combining high energy storage densities and

* Corresponding authors.
E-mail addresses: danny.mueller@tuwien.ac.at (D. Müller), peter.e163.weinberger@tuwien.ac.at (P. Weinberger).

https://doi.org/10.1016/j.apenergy.2021.116470
Received 5 October 2020; Received in revised form 31 December 2020; Accepted 8 January 2021
Available online 18 January 2021

cycle stabilities were found. For metal chlorides, during the charging / discharging cycles in the presence of ammonia slow degradation and evaporation of the materials was observed. This issue was circumvented by reducing the operating temperature and cycling between different degrees of ammoniation, *e.g.* in the case of $NiCl_2$ by cycling between $[Ni(NH_3)_2]Cl_2$ and $[Ni(NH_3)_6]Cl_2$. In contrast, sulphates are perfectly stable under all investigated conditions. The combination of $CuSO_4$ and NH_3 provided the most promising result directing towards applicability, as the high energy storage density of 6.38 GJ m^{-3} is combined with full reversibility of the storage reaction and no material degradation over cycling. The results of this comparative systematic material evaluation encourage for a future consideration of the so far underrepresented transition metal ammoniates as versatile thermochemical energy storage materials.

1. Introduction

The major challenge to integration of renewable and sustainable energy sources into the existing energy supply chain is effective compensation for temporal differences in peak energy production and demand [1]. This difficulty is especially acute in combination with fluctuating energy sources like the sun, for which non-operational times at night or during harsh weather conditions often correspond to peak demands, amplifying the mismatch between production and consumption [2,3]. Although, with *e.g.* pumped storage for hydropower already green energy storage technologies are available [4,5] and there exist other very promising approaches to thermal energy harvesting as *e.g.* thermoelectric [6] and thermomagnetic approaches, [7] storage of excess solar heat for use during low-production times demands for novel efficient thermal energy storage concepts. [8] Similarly, effective energy storage is required for heat recovery systems, designed to utilize (industrial) waste heat [1,2]. In other words, effective matching of energy supply to demand is strongly dependent on the availability and development of efficient heat storage technologies.

Several heat storage strategies have been proposed and investigated [3,9]. The most important concepts include sensible, [9] latent [10] and thermochemical [11,12] (sorption and reaction) heat storage. The storage capacity of these technologies increases in the scheme shown in Fig. 1 from left to right, however, their level of technological development is reversed.

Thermal storage systems operated commercially today include sensible [13–16] and, in some rare cases, latent thermal storage systems [10]. In a sensible energy storage cycle big volumes of a liquid (water, oil, molten salt, …) or solid (sand, concrete,…) storage material are heated, afterwards releasing the stored heat for further utilization. For a latent heat storage system, the storage material allows for a phase-change (solid–liquid, or liquid–gas), those inherent energy uptake or release is used to store or release heat. Both storage concepts suffer from the necessary thermal insulation to minimize heat losses during storage due to radiation [12]. Especially for sensible storage thermochemical systems could provide in some cases an attractive alternative, avoiding principal drawbacks of sensible systems including corrosiveness of the working medium or heat loss combined with potential crystallization of the melt in the system [17–20].

A very illustrative example of the necessary expenditures for a storage capacity of 10 GJ using the various available storage technologies was given by Luo et al. demonstrating, that 1 m^3 of thermochemical storage material can replace up to 34 m^3 of sensible heat storage medium [21].

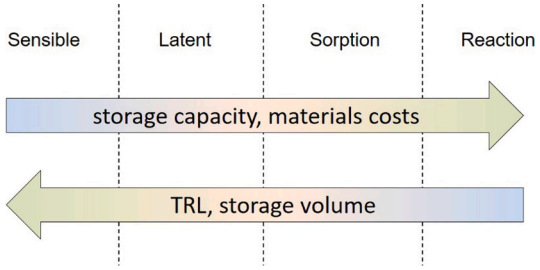

Fig. 1. Schematic comparison of storage capacity, materials costs, technology readiness level (TRL) and necessary storage volume for different thermal energy storage concepts.

In thermochemical systems the storage material is charged by a reversible chemical decomposition of material *A* during an endothermic decomposition reaction:

$$A_{solid} + heat \leftrightarrow B_{solid} + C_{gas}\uparrow$$

The charged material *B* is stored separately from the reactive gas *C* formed during the decomposition of *A*. To release the stored energy, *B* is reacted with gas *C*, reforming the initial storage material *A* [11,12]. This concept allows for the highest possible storage capacities, lossless (long-term) storage without thermal insulation and a broad, tuneable range of operational temperatures depending on the storage reaction applied [22]. The drawbacks currently preventing application include issues of cycle stability, reaction rate and material investment costs. Assessment of many potentially suitable materials reveals slow decomposition during cycling or slow reaction rates for the discharging step, therefore, eliminating them from potential thermochemical application. Material costs are considerably larger than for sensible storage material such as water, however, this factor may be mitigated by larger storage capacities, faster reaction times during charging and discharging and reduced overall investment costs due to smaller and mechanically simpler storage systems. In summary, the ideal thermochemical storage material would preferably provide high energy storage density at moderate material costs, perfect cycle stability without any degradation effects and fast charging and discharging reactions. Their potential is highlighted in several review articles [9,10], covering specific topics as solar thermal storage [8,23,24], or thermochemical energy storage in general [22,25].

The most common thermochemical energy storage materials include hydrates and hydroxides [26–29], hydrides [30,31], oxides [32–34], and carbonates [35–37]. Salt hydrates and hydroxides, using H_2O as a reactive medium, operate at temperatures up to a few hundred degrees and thus find potential application mainly in civil environments, including household heating or heat pumping [38]. Depending on the metal used, hydrides can be highly flexible when specifically designed for particular applications. Materials having their equilibrium temperature between 25 and 100 °C may be used for near ambient (housing) applications, whereas hydrides featuring storage temperature well above 100 °C could be used in concentrating solar power plants [39]. State of the art thermal storage systems suitable for combination with solar thermal systems have been extensively reviewed. In the case of combination with (concentrating) solar thermal systems, reversible redox-cycles of metal oxides [40–45], and, to a minor extent, metal hydride systems, have been investigated [30,31]. Metal oxides might be especially appropriate for higher reaction / storage temperatures, as well as attractive energy densities and reaction rates under safe reaction conditions [46]. Oxides are superior to carbonates in terms of reactive gas, since the discharging reaction may be carried out with ambient air, whereas carbonates release CO_2 during discharging, which should be stored for later use. However, it has recently been shown that carbonation reactions may also be operated at lower temperatures under increased CO_2 partial pressures, broadening their scope of application

[47].

Classifying potential materials for thermochemical energy storage according to the involved reactive gas shows, that ammonia was widely neglected so far. Efforts including ammonia focused mainly on Haber-Bosch type chemistry, forming and decomposing ammonia from and to elemental N_2 and H_2 in solar power plants [48,49]. Theoretical studies encompassing calculations of the energetic aspects of such applications [50–54], as well as first experimental prototypes [55–57] for energy storage purposes have been published.

Less attention was paid to the coordinating ability of the electron lone pair of the central nitrogen atom in NH_3, which is well known and leads to reaction with a wide variety of (transition) metal salts. Such reactions of (anhydrous) (transition) metal salts with ammonia result at least theoretically in an exothermic reaction, providing exceptionally high predicted energy storage densities [58]. However, only a very few practical studies of ammonia-compounds for thermochemical energy storage have been reported: Pioneering work dates to the 1980s by Ervin [43] and Dunlap [59], who describe experiments on alkaline-earth ammoniates and transition metal ammoniates, with a focus on $CoCl_2$ [60,61] and $MnCl_2$ [62]. Interest in alkaline earth chlorides for ammonia adsorption has been rekindled in the recent years and Van der Pal has published a performance-analysis of the $CaCl_2$ - NH_3 system on a 1 kg scale in an expanded natural graphite matrix to enhance thermal conductivity [63]. A coefficient of performance (COP) of 0.35–0.40 was found and a reasonable performance for a future scale-up to industrial levels is expected. Aristov and co-workers investigated γ-Al_2O_3 and vermiculite as support materials and found COPs between 0.40 and 0.48 and postulated reasonable potential for application in low-temperature driven cooling units [64]. Rosen has also recently reported on $SrCl_2$-NH_3 for thermochemical storage of solar heat [65]. Further studies on alkaline-earth ammoniates have been directed toward ammonia separation and storage [66], or for environmentally improved vehicles. A recyclable $DeNO_x$-system providing rapid NH_3-uptake and efficient liberation on demand that can be operated continuously has been developed [67,68]. Also for various nickel halides a similar effect was reported [69]. With exception of the historical reports [43,59], the investigation of $MnCl_2$ [70], and the combination of transition metal chlorides with alkaline earth chlorides [71], a systematic approach to the investigation of the energetics of transition metal ammoniates had yet to be undertaken.

We report herein the first systematic materials survey on the reaction of solid hydrous and anhydrous transition metal chlorides and sulphates with gaseous ammonia, aiming for high performing novel thermochemical energy storage materials. Reversibility of the ammoniation reaction, cycle stability, as well as determination of the experimental energy storage density by differential scanning calorimetry are used to verify the suitability of the reaction for thermochemical energy storage purpose.

The results suggest that the best systems examined possess a significantly higher experimental energy storage density in the temperature range from 25 to 350 °C than current state-of-the-art systems [72].

2. Experimental methodology

2.1. Material

All transition metal salts – both hydrated and anhydrous – were obtained commercially from Sigma Aldrich Austria in a purity greater than 99.9% and used as supplied. Before measurement, the materials were ground if necessary. For all samples, a sieved fraction smaller than 100 μm was used for the measurements. Ammonia (99.98%) was obtained from Messer.

2.2. Thermal analysis

For thermal analysis a Netzsch TGA/DSC 449C Jupiter® instrument equipped with a water vapour furnace including an air-cooled double jacket was used (see Fig. S1). The oven operates between 25 and 1250 °C, regulated by an S-type thermocouple. For determination of the energy contents at room-temperature the NH_3 gas flow was set to 100 ml min^{-1} allowing for a rapid and complete exchange of the atmosphere in the oven. The flow was controlled by Vögtlin Instruments “red-y” mass flow controllers. The transition metal salt (10 mg) was placed in an open aluminium crucible and reacted after 10 min of stabilization under N_2-atmosphere with NH_3 until the exothermic reaction had ceased. The DSC was calibrated according to the procedure suggested by Netzsch, using the In, Sn, Bi, Zn, Al and Ag standards provided by the manufacturer. Before each experiment a baseline-correction using the measurement software was performed.

For decomposition and cycling experiments, a sample mass of approximately 5 mg in an open alumina crucible was used, applying heating and cooling rates of 10 °C min^{-1} under an NH_3 atmosphere created by a constant 20 ml min^{-1} flow of NH_3 gas, controlled by Vögtlin Instruments “red-y” mass flow controllers. The heating/cooling rate of 10 °C min^{-1} was selected in the context of this general materials investigation to ensure reasonable measurement times, allowing contemporaneously for reasonable accuracy of the results [73]. For specific purposes and later on additional measurements heating/cooling rates of 5 or 2 °C min^{-1} could be suitable. Prior to all measurements a thermal correction was performed. To determine the decomposition (deamination) temperature of the various transition metal complexes, the fully ammoniated transition metal salt was heated to 450 °C. For the cycling experiments, after a 10 min stabilization time under NH_3-atmosphere at room-temperature the samples were heated slightly over the before determined decomposition temperature, ensuring complete thermal deamination of the material. Then a cooling phase under NH_3 atmosphere was followed by an isothermal stabilization time of 30 min at room-temperature, before the heating/cooling cycle was repeated.

Evaluation of the TGA and DSC curves was performed with the Netzsch Proteus – Thermal Analysis – 6.0.0 software package. Mass-losses, residual mass, DSC-values and onset temperatures were calculated from the respective area of the baseline-corrected measurement data by the software algorithms. The mass-loss is given in % and was obtained by subtracting the residual mass (in %) determined by the software analysis-algorithm from the original mass (100%). Experimental error is given according to the instruments’ specification.

2.3. X-Ray powder diffraction (P-XRD)

The powder X-ray diffraction measurements were carried out on a PANalytical X’Pert Pro diffractometer in Bragg-Brentano geometry using Cu $K_{\alpha 1,2}$ radiation and an X’Celerator linear detector.

2.4. Scanning electron microscopy (SEM)

SEM images were recorded on a Quanta SEM instrument from FEI under low-vacuum and in the presence of water vapor to prevent electrostatic charge. The samples were mounted on carbon pellets on top of the sample holder and plasma vacuum deposition was used to coat the samples with a thin layer of gold to ensure appropriate conductivity. The gold coating was performed using an AGAR sputtering system at 10 mA for 30 s.

3. Results and discussion

The coordination chemistry of transition metal salts with ammonia is known since the pioneering work of Alfred Werner at the early beginning of the 20th century. Although the reaction of ammonia, coordinating to transition metal ions as *e.g.* Cu^{2+}, Co^{2+} and Ni^{2+} is well-studied and highly exothermic [74], studies of thermochemical energy storage systems utilizing transition metal ammoniates are limited. Among other reasons, this may be attributed to the rather exotic nature of this

combination, and more importantly, eventual reservations about working with (pressurized) ammonia at elevated temperatures·NH_3 as generally toxic gas will not be the first choice for *e.g.* large applications in urban environment or households. Nevertheless, NH_3 is widely applied in closed systems for *e.g.* industrial cooling systems, carefully preventing any release and harm to the environment. Also the issue of its corrosiveness becomes less relevant, when preventing the presence of moisture. There are sufficient materials at hand, withstanding the combination of high temperatures, ammonia and metal salts. Therefore, with sufficient and proper safety measures in place, the combination of transition metal salts and ammonia as thermochemical energy storage material becomes feasible.

Starting from a systematic analysis of the HSC-chemistry thermochemical database entries it becomes evident, that several so far non-investigated combinations between anhydrous (transition) metal salts and NH_3 as reactive gas could be attractive candidates for thermochemical energy storage (TCES) materials in solid–gas reactions [58]. Additional to the list of candidates extracted from the HSC-database search, further transition metal salts known for their ammonia-complexes (*e.g.* Mn^{2+}, $Fe^{2+/3+}$, Co^{2+}, Ni^{2+}, Cu^{2+}, Zn^{2+}) were selected for investigation of their reaction with gaseous NH_3. As it is known, that depending on the coordinating nature of the counter-anion reactivity and therefore thermodynamic parameters differ, additional to chloride also sulphates – if commercially available to reasonable prices – were chosen.

Differential scanning calorimetry (DSC) under an NH_3 atmosphere at 25 °C was used to determine the heat of reaction for the formation of the ammoniate-complexes. During the reactions it was observed, that all investigated materials feature fast reaction rates, completing the formation of the ammoniate-complexes under the measurement conditions (visible by no further heat evolution) within less than 10 min. As several of the salts investigated are available in both anhydrous and variously hydrated forms, the most common hydrate species were also investigated regarding their reactivity towards NH_3. In Fig. 2 the reaction enthalpy, thus the energy content, is given for all investigated materials – in Fig. 2a for the anhydrous salts, in Fig. 2b for their hydrated forms. The materials are ranked by gravimetric energy content (kJ/kg; blue) with the molar energy content (kJ/mol; green) adjacently reported for completeness and convenience.

From the anhydrous materials investigated, the largest enthalpy of reaction was observed for $NiCl_2$ forming its hexaammine-complex, liberating 2464 kJ kg^{-1} during ammoniation. Considering the bulk density of the anhydrous material (3.55 t m^{-3}) [75], this results a calculated potential maximal storage capacity of 8.75 GJ m^{-3} of the material. For the investigated sulphates the largest heat of reaction was measured for $CuSO_4$, forming the tetraammine-complex reacting with NH_3 (entry 5, 6.38 GJ m^{-3} based on a bulk density of 3.6 t m^{-3} [75]). In Fig. S2 the entries from Fig. 2 are sorted according to the molar energy content, resulting in a shifted weighting towards salts with a higher molecular weight, especially in the case of the hydrates. The exact values for both energy content in kJ kg^{-1} and kJ mol^{-1}, as well as the energy density in GJ m^{-3}, are given in Table S1 enabling ready comparison and assessment of the potential volumetric efficiency of the materials studied.

Based on the theoretical predictions derived from the HSC-chemistry database, also Pd^{2+}, Pt^{2+}, Cd^{2+}, Sc^{3+}, and Ce^{3+} should react highly exothermic with NH_3 [58]. In contrast, the experimental values shown in Fig. 2 evidence, that Pd^{2+}, Pt^{2+}, Cd^{2+}, Sc^{3+}, and Ce^{3+} are not comparable to the investigated first-row transition metals in terms of reaction enthalpy, not matching with the prediction from the database. Therefore, as well as based on their price and toxicity in the case of Cd^{2+}, they were excluded from further investigations. The reason for this contrasting experimental behaviour is found in the case of the rare-earth elements (Sc^{3+} and Ce^{3+}) in their dominating oxophilicity, preferring O-donor sets above N-donors as *e.g.*·NH_3. Additionally, the contribution of the lattice enthalpy is in the case of three-valent cations larger than for divalent ones, so the enthalpy of reaction with NH_3 is no longer large enough to result high overall enthalpies of reaction. For the divalent cations Pd^{2+}, Pt^{2+}, Cd^{2+} a suitable explanation is found according to the hard and soft acid and base concept (HSAB-concept, Pearson concept) [74], favouring pairs of hard acids and hard bases, or weak acids and weak bases. Pd^{2+}, Pt^{2+}, Cd^{2+} are generally classified as weak acids, whereas NH_3 falls in the category of hard bases, explaining with this "mismatch" of a weak acid and hard base the measured low enthalpy of reaction.

For each selected transition metal cation in addition both the counter anion and degree of hydration impact on the reaction enthalpy, thus on the energy storage capacity of the material. Having this in mind, enthalpies of ammoniation were compared for chlorides and sulphates, as well as for the most common hydrates of the transition metal salts. Transition metal sulphates typically yield reaction enthalpies of 20–100 kJ mol^{-1} lower than the chlorides. This is attributed to the stronger electrostatic interactions between divalent cations and divalent anions, which tend to prevent saturation of the metal-cation coordination sphere with ammonia ligands [76]. Taking Ni^{2+} or Cu^{2+} as an example, for both chlorides the corresponding hexaammine-complex $[M(NH_3)_6]Cl_2$, M = Ni^{2+}, Cu^{2+} is formed, whereas for the sulphates only the tetraammine-complex $[M(NH_3)_4]Cl_2$, M = Ni^{2+}, Cu^{2+} is obtained.

Also, the initial salt hydration state affects the heat storage capacity of transition metal salts. The reasoning for this observation is detailed in

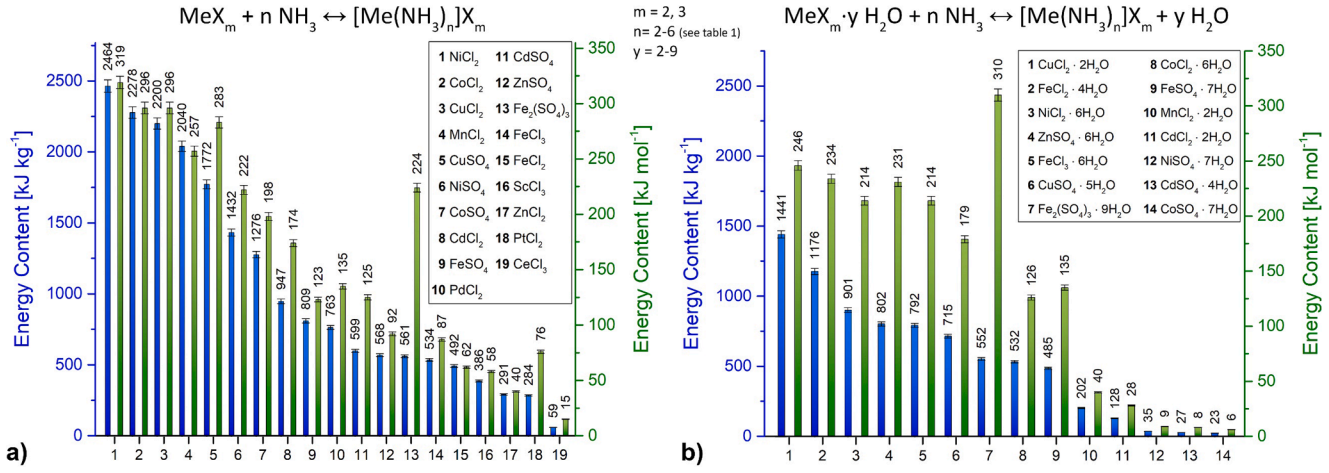

Fig. 2. Energy of reaction of selected (transition) metal salts with NH_3 at 25 °C. a) Anhydrous salts b) Most common hydrates. Exemplarily, the TGA/DSC curves for $CuSO_4$ + 4 NH_3 ↔ $[Cu(NH_3)_4]SO_4$ is given in the supporting information(see Fig. S3).

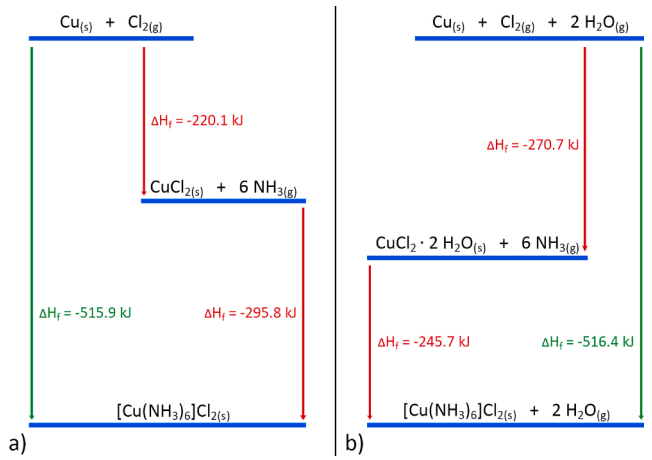

Fig. 3. Schematic comparison of the heats of formation for a) anhydrous $CuCl_2$ and b) $CuCl_2{\cdot}2H_2O$ and the further reaction with NH_3 to the $[Cu(NH_3)_6]Cl_2$-complex. ΔH_f $CuCl_2$ / $CuCl_2{\cdot}2H_2O$ was taken from the NBS tables of chemical thermodynamic properties[31]; and $\Delta H_f[Cu(NH_3)_6]Cl_2$ was determined in this work. Ammoniation of anhydrous $CuCl_2$ is shown on the left (Fig. 3a) and $CuCl_2{\cdot}2H_2O$ on the right (Fig. 3b).

Fig. 3 as schematic representation of the heats of formation for $[Cu(NH_3)_6]Cl_2$, starting from anhydrous $CuCl_2$ and the dihydrate $CuCl_2{\cdot}2H_2O$.

The reaction steps from copper to the final $[Cu(NH_3)_6]Cl_2$-complex are all exothermic. Since the molar heat formation of $CuCl_2{\cdot}2H_2O$ is significantly more negative (−270.7 kJ/mol) than that of anhydrous $CuCl_2$ (−220.1 kJ/mol), the ligand-exchange reaction of $CuCl_2{\cdot}2H_2O$ with NH_3 (see Fig. 2) results in a smaller change in enthalpy than observed for anhydrous $CuCl_2$. For both pathways, combining the literature values for the ΔH_f $CuCl_2$ / $CuCl_2{\cdot}2H_2O$ [77] with the enthalpy of reaction forming $[Cu(NH_3)_6]Cl_2$ determined in the present work, one can find a perfect agreement with the calculated $\Delta H_f = -516$ kJ mol^{-1}.

The exothermic reaction between the metal salt and NH_3 corresponds to the discharging reaction of a TCES material. Charging the material through thermal decomposition of the ammoniate-complex results in the anhydrous material, regardless of the hydration state of the initial precursor material. Therefore, on repeated operation of the TCES-process, the lower energy capacity of hydrated salts accounts only in the first cycle, from the second cycle on, the reaction enthalpy is equivalent to the one measured when starting from the anhydrous material. Once the hydrate water is fully removed after the first charging / discharging cycle, the performance and storage capacity of the initial anhydrous or hydrous transition metal salt are identical. In Fig. 4 this behaviour is exemplified for the case of $CuSO_4{\cdot}5H_2O$: Before initiating the first discharging / charging cycle, $CuSO_4{\cdot}5H_2O$ is reacted with ammonia at room-temperature (the initial reaction with NH_3 is omitted in Fig. 4). This hydrated ammoniate-complex, resulting directly from $CuSO_4{\cdot}5H_2O$, is subsequently cycled under NH_3-atmosphere.

During the first complete discharging / charging cycle residual H_2O is removed from the system, causing the mass-loss between the initial mass and the subsequent maxima. Therefore, as shown in Fig. 4, the first cycle shows a slightly different thermal behaviour. In the case of $CuSO_4$ this is seen in the rather gradual, than clear stepwise NH_3 removal or uptake, observed during the further cycles. Starting with the second cycle, the discharging and charging profiles are highly comparable in all subsequent cycles in terms of mass-changes, onset-temperatures, and reaction enthalpies. The observed overall mass-change of 28% in each cycle is in reasonable agreement with the expected theoretical change of 29.9% for the reaction $[Cu(NH_3)_4]SO_4 \leftrightarrow CuSO_4 + 4\ NH_3$.

A TCES material should preferably not only provide a high energy storage density, but even more important, allow for fully reversible discharging / charging over many cycles, enabling long-term application in a system. From all investigated materials $NiCl_2$ revealed the highest enthalpy of reaction with NH_3 (see Fig. 2a). It was the first material being investigated for reproducibility and cycle stability over targeted 10 cycles in the TGA/DSC, varying the temperature between 25 and 400 °C. The result is given in Fig. 5a revealing, that already after the first cycle 5.4% of the initial $NiCl_2$-mass were lost. The mass-loss continued during subsequent cycling and worsened, until after interrupting the cycling test after the seventh repetition, a final loss of 25.2% (Fig. 5a) was calculated.

The reason for this continuous loss of $NiCl_2$ is thought as combination of transport phenomena and reduction of $NiCl_2$ on heating under NH_3 atmosphere. After the 7th cycle, the formerly yellow material had darkened and traces of NH_4Cl were identified in the powder diffraction of the material. In addition, on the sample holder of the TGA/DSC system a dark layer had deposited around the crucible. The slow decomposition observed in the case of $NiCl_2$ was also observed during cycling experiments with $CoCl_2$ and $CuCl_2$ shown in Figs. S4 and S5, although to a markedly lesser degree ($CoCl_2$ 2.1%, $CuCl_2$ 3.2%). This effect is

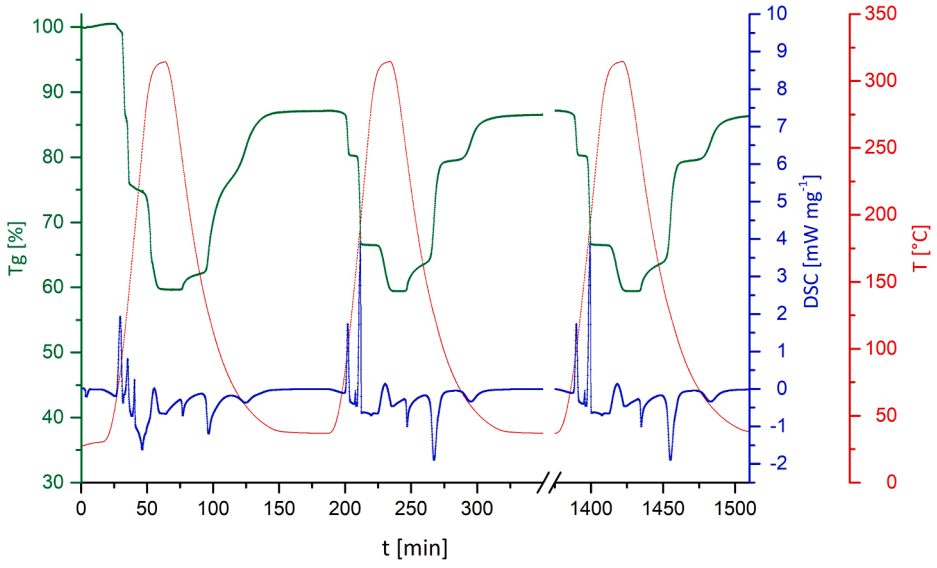

Fig. 4. Cycling experiment with $CuSO_4{\cdot}5H_2O$. During the first complete charging / discharging the former hydrate water is removed from the system, resulting a stable and reproducible performance from the second cycle on. For comparison, after stability is achieved only the 10th cycle is represented.

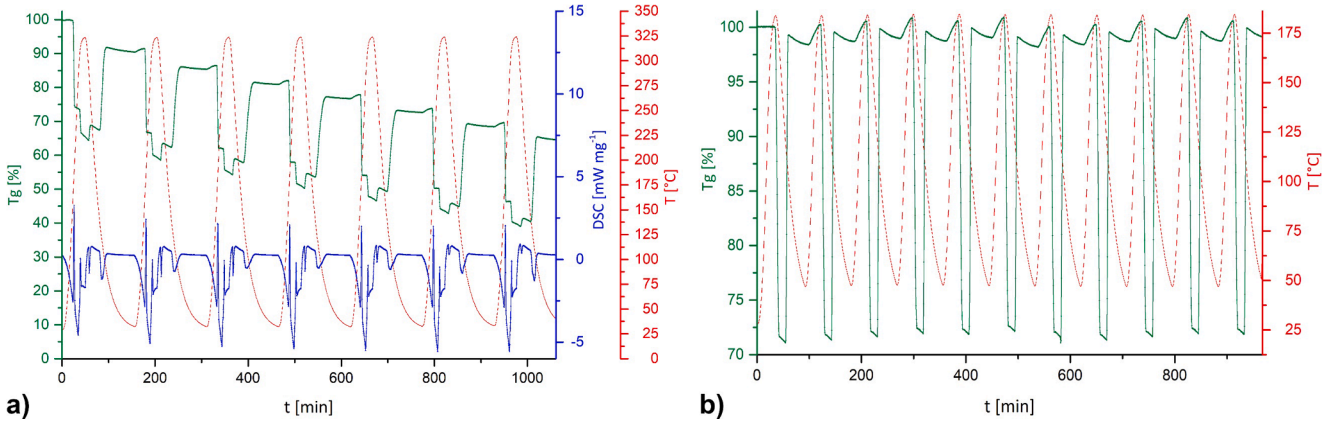

Fig. 5. a) Loss of $NiCl_2$ during cycle-stability tests. Within 7 consecutive cycles 25.2% of the initial $NiCl_2$ is lost. b) Loss of $NiCl_2$ during cycle-stability tests if the decomposition temperature is lowered to cycle between $[Ni(NH_3)_2]Cl_2$ and $[Ni(NH_3)_6]Cl_2$. Under the refined conditions the reaction is cycle-stable.

attributed to decreased thermal stability of the metal chlorides under a combination of high temperatures and an atmosphere of ammonia. To prevent this gradual decomposition in the case of the chlorides by lowering the maximal decomposition temperature in the experiment only a partial deamination, stabilizing the storage material by one or more residual NH_3-ligands, could be beneficial. In this case, the complete storage capacity of the system is sacrificed to enhance cycle stability. A cycling experiment using an adapted temperature program for the $NiCl_2$ case is given in Fig. 5b. If the deamination temperature is limited to 180 °C, the diammine-complex $[Ni(NH_3)_2]Cl_2$ rather than $NiCl_2$ is obtained as charged species in the process. Cooling under an NH_3 atmosphere results in reformation of the hexaammine compound $[Ni(NH_3)_6]Cl_2$. This limitation results a fully stable discharging / charging cycle, invariant over the 10 cycles shown in Fig. 5b. This observation is supported by previous work in which the thermal decomposition of $[Ni(NH_3)_6]Cl_2$ resulting the diammine complex $[Ni(NH_3)_2]Cl_2$, was reported. [78] The reversible process $[Ni(NH_3)_6]Cl_2 \leftrightarrow [Ni(NH_3)_2]Cl_2 + 4NH_3$ demonstrates, that taking into account the trade-off of a lower overall storage density allows also for transition metal chlorides a reversible and cycle-stable application.

The release of NH_3 during heating (charging) of the chloride-complexes occurs mostly continuous. In contrast, for the sulphates a stepwise NH_3-release is observed. Missing thermal plateaus, where the deammination would stop at a defined species, even careful control of the deamination temperature cannot fully prevent slight decomposition effects in the case of the chlorides over long-term cycling. This differing thermal decomposition behaviour is shown exemplarily for $[Cu(NH_3)_6]Cl_2$ and $[Cu(NH_3)_4]SO_4$ in Fig. 6.

In Fig. 6a the highlighted area during the mass loss corresponds to the continuous and gradual mass-loss before and after the thermal dissociation of the last NH_3-ligand in $[Cu(NH_3)_6]Cl_2$. In contrast, in Fig. 6b in the case of $[Cu(NH_3)_4]SO_4$ there is a slight gradual plateau before the steep drop, the latter corresponding to the irreversible decomposition of the material. Careful temperature control in this case allows for stabilization of the anhydrous $CuSO_4$-phase. Another option preventing the degradation of the material could be purging of the system with N_2 to remove the NH_3 liberated during thermal decomposition. However, studies under a static NH_3 atmosphere most closely emulate the conditions anticipated for industrial application, under which the inherent toxicity of NH_3 would be mitigated by operating a closed system.

In the case of the transition metal sulphates, no decomposition during cycling was observed (for example, Fig. S6 for 10 charging / discharging cycles with $CuSO_4$). Although, the chlorides would provide maximal energy storage densities, based on the results of the cycle stability tests transition metal chlorides are under the conditions investigated unsuitable in a real application as thermochemical energy storage material.

To investigate the discharging / charging behaviour of the various materials, all materials included in the systematic study were subjected two consecutive charging / discharging cycles under an atmosphere of NH_3 in the TGA/DSC. The results for each material are detailed in the supporting information, Figs. S7–S16. The decomposition and formation temperatures of the ammoniate-complexes, as well as the associated energies are reported in Table 1. For all materials showing an identical first and second cycle, in Table 1 the results for the second cycle are

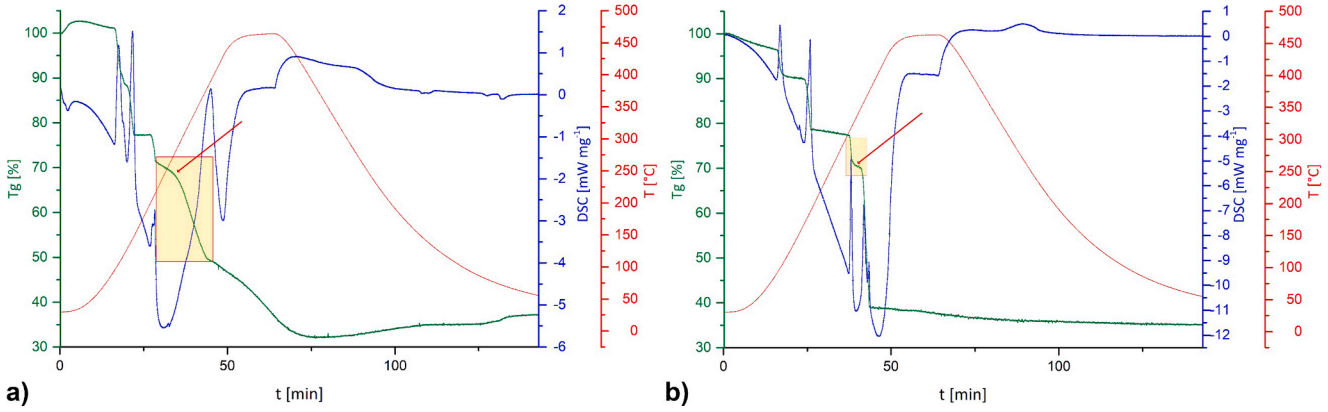

Fig. 6. a) Decomposition of $[Cu(NH_3)_6]Cl_2$ under NH_3 atmosphere, continuous gradual mass-loss before and after removal of the last NH_3-ligand. b) Decomposition of $[Cu(NH_3)_4]SO_4$ under NH_3 atmosphere, plateau-phase during removal of the last NH_3-ligand.

Table 1
Decomposition / formation temperatures and associated energies for the investigated transition metal ammoniates.

	$[Ni(NH_3)_6]Cl_2$		$[Co(NH_3)_4]Cl_2$		$[Cu(NH_3)_6]Cl_2$	
	charging	**discharging**	**charging**	**discharging**	**charging**	**discharging**
	T [°C] / E [kJ kg^{-1}]	T [°C] / E [kJ kg^{-1}]	T [°C] / E [kJ kg^{-1}]	T [°C] / E [kJ kg^{-1}]	T [°C] / E [kJ kg^{-1}]	T [°C] / E [kJ kg^{-1}]
1st step	176.3 / 802.4 ± 22.5	274.0 / −133 ± 3.7	140.0 / 743 ± 13.4	56.4 / −807 ± 10.5	99.8 / 320 ± 5.8	—
2nd step	309.9 / 374.1 ± 12.0	139.6 / −1289 ± 23.2	—	—	133.5 / 366 ± 6.6	—
3rd step	—	—	—	—	296.6 / 1199 ± 38.4	—
	$[Mn(NH_3)_2]Cl_2$		$[Cu(NH_3)_4]SO_4$		$[Ni(NH_3)_4]SO_4$	
	charging	**discharging**	**charging**	**discharging**	**charging**	**discharging**
	T [°C] / E [kJ kg^{-1}]	T [°C] / E [kJ kg^{-1}]	T [°C] / E [kJ kg^{-1}]	T [°C] / E [kJ kg^{-1}]	T [°C] / E [kJ kg^{-1}]	T [°C] / E [kJ kg^{-1}]
1st step	87.5 / 846 ± 15.2	60.8 / −2005 ± 36.1	79 / 180 ± 3.2	66 / −153 ± 2.8	119.3 / 598 ± 10.8	127.1 / −378 ± 6.8
2nd step	249.3 / 581 ± 16.3	—	168 / 444 ± 8.0	138 / −479 ± 8.6	—	—
3rd step	—	—	307 / 443 ± 14.2	248 / −247 ± 6.9	—	—
	$[Co(NH_3)_4]SO_4$		$[Cd(NH_3)_4]Cl_2$		$[Fe(NH_3)_2]SO_4$	
	charging	**discharging**	**charging**	**discharging**	**charging**	**discharging**
	T [°C] / E [kJ kg^{-1}]	T [°C] / E [kJ kg^{-1}]	T [°C] / E [kJ kg^{-1}]	T [°C] / E [kJ kg^{-1}]	T [°C] / E [kJ kg^{-1}]	T [°C] / E [kJ kg^{-1}]
1st step	101.7 / 268 ± 4.8	80.2 / −1026 ± 18.5	58.5 / 372 ± 6.7	—	79.5 / 441 ± 7.9	—
2nd step	132.1 / 332 ± 5.0	—	237.9 / 236 ± 6.6	—	231.2 / 198 ± 5.5	—
3rd step	260.3 / 307.4 ± 5.5	—	—	—	—	—
4th step	293.2 / 258 ± 8.3	—	—	—	—	—
	$[Cd(NH_3)_2]SO_4$		$[Zn(NH_3)_4]SO_4$		$[Zn(NH_3)_4]Cl_2$	
	charging	**discharging**	**charging**	**discharging**	**charging**	**discharging**
	T [°C] / E [kJ kg^{-1}]	T [°C] / E [kJ kg^{-1}]	T [°C] / E [kJ kg^{-1}]	T [°C] / E [kJ kg^{-1}]	T [°C] / E [kJ kg^{-1}]	T [°C] / E [kJ kg^{-1}]
1st step	85.6 / 314 ± 5.7	163.5 / −226 ± 4.1	79.0 / 27 ± 0.5	105 / −761 ± 13.7	94.8 / 27 ± 0.5	235.0 / −71 ± 2.0
2nd step	200.4 / 585 ± 16.4	65.1 / −490 ± 8.8	108.0 / 202 ± 3.6	—	247.0 / 58 ± 1.6	—
3rd step	—	—	174.0 / 243 ± 4.4	—	—	—
4th step	—	—	215.0 / 343 ± 9.6	—	—	—
	$[Cu(NH_3)_6]Cl_2$ from $CuCl_2\ 2H_2O$		$[Fe(NH_3)_3]Cl_2$ from $FeCl_2\ 4H_2O$		$[Cu(NH_3)_4]SO_4$ from $CuSO_4\ 5H_2O$	
	charging	**discharging**	**charging**	**discharging**	**charging**	**discharging**
	T [°C] / E [kJ kg^{-1}]	T [°C] / E [kJ kg^{-1}]	T [°C] / E [kJ kg^{-1}]	T [°C] / E [kJ kg^{-1}]	T [°C] / E [kJ kg^{-1}]	T [°C] / E [kJ kg^{-1}]
1st step	103.0 / 265 ± 4.8	134.1 / −74 ± 1.3	117.3 / 776 ± 14.0	127.4 / −1350 ± 24.3	98.4 / 200 ± 3.6	248.0 / −161 ± 4.5
2nd step	137.3 / 299 ± 5.4	104.8 / −310 ± 5.6	283.1 / 178 ± 5.7	—	173.2 / 456 ± 8.2	136.0 / −629 ± 11.3
3rd step	291.8 / 369 ± 11.8	—	—	—	308.4 / 246 ± 8.1	66.5 / −175 ± 3.2
	$[Fe(NH_3)_2]SO_4$ from $Fe_2(SO_4)_3\ 9H_2O$		$[Mn(NH_3)_2]Cl_2$ from $MnCl_2\ 2H_2O$		$[Cd(NH_3)_2]SO_4$ from $CdSO_4\ 4H_2O$	
	charging	**discharging**	**charging**	**discharging**	**charging**	**discharging**
	T [°C] / E [kJ kg^{-1}]	T [°C] / E [kJ kg^{-1}]	T [°C] / E [kJ kg^{-1}]	T [°C] / E [kJ kg^{-1}]	T [°C] / E [kJ kg^{-1}]	T [°C] / E [kJ kg^{-1}]
1st step	137.6 / 88 ± 1.6		91.2 / 414 ± 7.5	61.3 / −949 ± 17.1	83.7 / 399 ± 17.1	160 / −296 ± 5.3
2nd step	—	—	—	—	206.7 / 258 ± 7.2	64.3 / −490 ± 8.8
3rd step	—	—	—	—	258.4 / 197 ± 5.5	—
	$[Co(NH_3)_4]SO_4$ from $CoSO_4\ 7H_2O$					
	charging	**discharging**				
	T [°C] / E [kJ kg^{-1}]	T [°C] / E [kJ kg^{-1}]				
1st step	111.6 / 678 ± 24.4	93.7 / 1048 ± 18.9				
2nd step	244.1 / 366 ± 10.3	—				
3rd step	—	—				

shown. If the discharging (thus reformation of the ammoniate) was incomplete (*e.g.* for $[Cd(NH_3)_4]Cl_2$, $[Fe(NH_3)_2]SO_4$, etc.), the data of the first cycle are given.

To proceed with a more detailed study, the initially investigated materials were narrowed down according to three parameters: a) reversibility of the ammoniation, b) energy content, c) toxicity and price. Although, careful selection of the deammoniation temperature and specific optimization of the process (*e.g.*in the case of $NiCl_2$ $[Ni(NH_3)_6]Cl_2 \leftrightarrow [Ni(NH_3)_2]Cl_2 + 4NH_3$) could allow also for good cycle stability of chlorides, they were excluded from a further investigation according to criterium a). Considering criteria b) and c), the initially 19 materials were narrowed down to $CuSO_4$, $CoSO_4$ and $ZnSO_4$ as the three most promising candidates.

All three materials were found fully cycle-stable over 10 cycles. Analysis of the powder X-Ray patterns of the materials before and after 10 cycles support the full reversibility identified by TGA/DSC, as no change in the phase composition (apart for $ZnSO_4$, where the $ZnSO_4{\cdot}H_2O$ was no longer present after 10 cycles of NH_3) was observed. In Fig. 7 exemplarily the P-XRD patterns for $[Cu(NH_3)_4]SO_4$ before and after 10 cycles is shown, the data for $CoSO_4$ (Fig. S17) and $ZnSO_4$ (Fig. S19) are given in the supplement.

For all three compounds a comparison of SEM images before and after the 10 cycles of NH_3 treatment show a tendency towards smaller particle sizes. This effect is explained by the volume work occurring

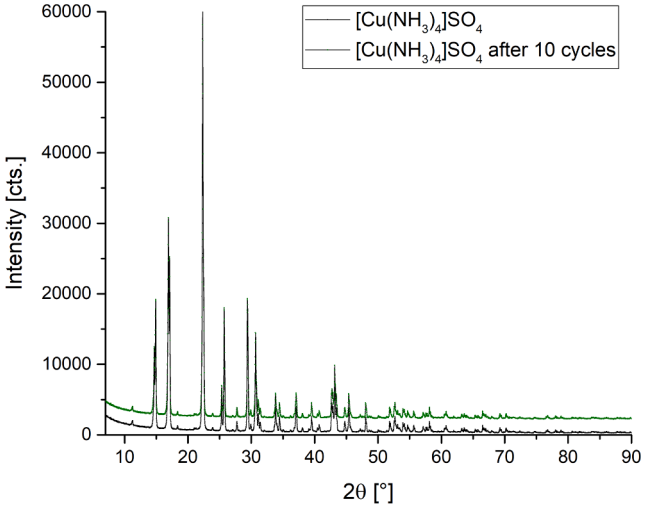

Fig. 7. P-XRD of $[Cu(NH_3)_4]SO_4$ before (black) and after (green) 10 heating / cooling cycles under NH_3 atmosphere.

during NH_3 coordination, resulting from significant expansion of the crystallographic lattice, and subsequent contraction upon NH_3 removal. Although, this volume work causes a fragmentation of the particles, the reactivity of the material seems unaffected – at least for the 10 cycles investigated within this study. In Fig. 8, exemplarily the SEM-images for $[Cu(NH_3)_4]SO_4$ before (Fig. 8a) and after (Fig. 8b) 10 cycles are shown, for $CoSO_4$ (Fig. S18) and $ZnSO_4$ (Fig. S20) the data are given in the supplement.

Full reversibility over 10 cycles is so far a very promising result within the scope of this systematic material comparison. For a final assessment on the long-term performance of the materials, within a subsequent study the long-term stability behaviour of the material over hundreds of cycles, avoiding a time-consuming TGA/DSC setup, will be necessary.

Comparing the final candidates assessed, $CuSO_4$ shows the best performance in the present study, both in terms of reversibility and energy content. Over the 10 cycles, as well as in the P–XRD no sign for decomposition, or changes of the material was found. With 6.38 GJ m^{-3} also the experimentally determined storage density is the highest after the sulphates. Additionally, it combines low toxicity and low prices, both relevant aspects for future application.

Although excluded during this study, a follow-up investigation on $CoCl_2$ could be attractive for two reasons: First, it has the second highest energy density from the 19 materials investigated and second, it seems promising as only slight decomposition during cycling was observed. Solutions to this issue could be a storage cycle avoiding an atmosphere of NH_3 during charging (thermal decomposition), or a careful fine-tuning of the thermal decomposition. A similar effort could also be applied to $CuCl_2$. To highlight this optimization potential the P-XRD data and SEM–images before and after 10 cycles are given for $CoCl_2$ (Figs. S21 and S22) and $CuCl_2$ (Figs. S23 and S24) in the supporting information. Both analyses show also for the chlorides a fragmentation of the particles due to the volume work during the NH_3 coordination and subsequent decomposition.

Within boundary conditions such as temperature range/equilibrium temperatures, as well as risks and costs associated with utilization of transition metals and ammonia, two distinct features of $CuSO_4$ and the other ammoniates stand-out in terms of applicability: The discussed high energy storage density and demonstrated rapid chemical reactions involved. Based on these aspects, transition metal ammoniates are the ideal match for any application demanding fast heat release/uptake and/ or confined space for the storage material. Two explicit examples should be given to highlight applicability: Solar thermal and mobile heat storage units.

Solar thermal power plants as *e.g.* Shams1 in Abu Dhabi include a fluid-circuit heated by the sun through reflectors, transferring the collected thermal energy through a heat exchanger. A certain minimum temperature (especially during night and before ramp-up before solar irradiation starts) must be maintained, otherwise the system may incur damage. The current setup relies on gas-firing to reach the ramp-up temperature in the morning or peaks in the heat-demand during non-operational times. As during day-time abundant thermal energy is available, a certain percentage could be stored thermochemically by *e.g.* decomposing $[Cu(NH_3)_4]SO_4$, allowing for fast liberation of the stored heat through reaction with NH_3 on demand for ramp-up in the morning and also for buffering peak demands. This would substitute the gas-firing, resulting in a completely sustainable solar thermal power plant. The reason for $CuSO_4$ being the ideal storage material for this purpose is based in both the fast heat liberation and the achieved high peak temperatures.

The second use-case for thermochemical energy storage systems based on ammoniates comes ironically from the oil and gas industry. The authors were approached by an important player of the international oil and gas industry, asking for a mobile solution of a heat storage system featuring fast heat-release with peak temperatures above 200 °C and the smallest possible dimensions/weight. In this case the main selling point would be the high energy storage density of *e.g.* 6.38 GJ m^{-3} for $CuSO_4$, then in combination with fast heat release and high peak temperature.

Although, no commercial application of thermochemical energy storage systems is currently on the market, the authors sense an increasing interest in this technology and are confident that within the next few years commercial applications will appear.

Compared to other state of the art salt thermochemical storage materials reported in literature (*e.g.* $SrBr_2{\cdot}6H_2O$), the candidates for thermochemical energy storage systems based on the reversible ammoniation of transition metal salts identified herein feature broader operational temperature profiles and higher experimental energy storage densities. A direct comparison of the storage efficiency is not possible, because the storage efficiency is defined as ratio of energy released from the storage system to the used and energy needed to charge the storage system [79], measured on a specific prototype-setup [80]. This accounts both for losses during the storage and the charge/ discharge cycle. Those data are so far not available for the herein reported systems, as in a fundamental study no prototype setup has been operated with the investigated materials. However, to allow for a rough estimation of potential efficiency, accounting for losses during the charge/ discharge cycle, for the most promising candidates identified during this study in Table 2 charging/discharging efficiencies calculated from the DSC-measurements during cycling are shown.

Considering the results of this first evaluation on storage efficiency

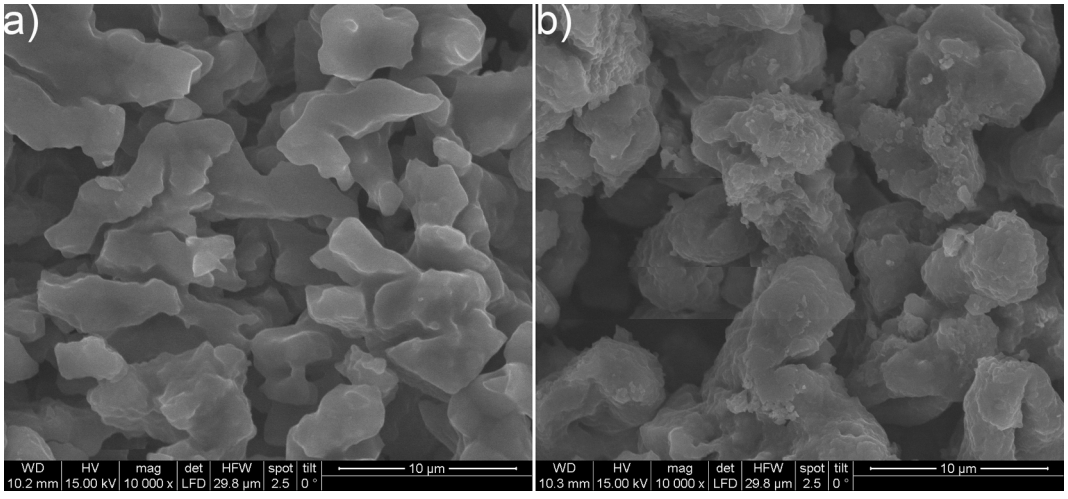

Fig. 8. SEM image of $[Cu(NH_3)_4]SO_4$ before (a) and after (b) 10 heating / cooling cycles under NH_3 atmosphere.

Table 2
Calculated storage efficiency/loss during cycling from DSC-measurements.

Material	Storage efficiency [%]	Loss [%]
$CuSO_4$	97.9	2.1
$CoSO_4$	96.0	4.0
$ZnSO_4$	68.7	31.3
$CoCl_2$	94.3	5.7
$CuCl_2$	42.5	57.5

the selection of most promising candidates is narrowed further, as only $CuSO_4$, $CoSO_4$ and $CoCl_2$ feature efficiencies on cycling greater than 90%. All further evaluation and subsequent comparison to the storage efficiency of other salt storage materials will be done in the prototyping phase.

4. Conclusion

Various transition metal salts are known to react readily and exothermic with ammonia. The herein presented systematic study on solid–gas reactions between transition metal chlorides and sulphates with ammonia sheds light on their applicability as thermochemical energy storage material. Starting point of the study was a short list of 17 transition metal chlorides and sulphates, as well as $ScCl_3$ and $CeCl_3$. This selection was based on thermodynamic data of the HSC-database, suggesting a good suitability for the targeted purpose and on coordination chemistry 'textbook-knowledge'.

The key-findings of this study can be summarized as follows:

1) All investigated metal salts react with ammonia, forming the corresponding NH_3-complexes
2) The reaction enthalpy is strongly dependent to the anion, oxidation state and 'hardness' of the metal ion according to the HSAB-concept. Chlorides provide generally higher enthalpies of reaction than sulphates. The highest energy density for the chlorides is found for $NiCl_2$ with 8.75 GJ m^{-3}, the highest for the sulphates for $CuSO_4$ with 6.38 GJ m^{-3}
3) The anion influences the cycle stability, as for the chlorides a higher tendency to decomposition or volatility during the thermal decomposition of the ammoniates under NH_3 atmosphere is observed. The sulphates show good cycle-stability over 10 cycles without indications of decomposition or changes of the material. For the chlorides it was demonstrated at the example of $NiCl_2$, that specific adaptation of the thermal decomposition, avoiding complete decomposition of the ammine-complex to an intermediate ammoniate ($[Ni(NH_3)_6]Cl_2 \leftrightarrow [Ni(NH_3)_2]Cl_2 + 4NH_3$) results in a cycle stabile process
4) Based on the present results $CuSO_4$ is identified as the most promising candidate, followed by $CoSO_4$ and $ZnSO_4$. A more detailed investigation / fine tuning of the thermal decomposition could also enable the application of $CoCl_2$ and $CuCl_2$
5) Hydrated transition metal salts can be used as economic starting material, as within the first ammoniation / deammoniation cycle the H_2O is removed and from the second cycle on the performance is identical to those of the initially anhydrous metal salts
6) A first comparison with other thermochemical energy storage materials operating in the same temperature window as the ammoniates shows, that they have a notable potential due to high storage densities, the discharging taking place starting already at room-temperature and their fast reactivity with NH_3
7) Within a next step, the long-term stability of the materials needs verification before subsequently considering scale-up in a prototype. Aspects needing an in-depth investigation after this initial material investigation include a detailed study on (eventual) degradation processes, the identification of a suitable reactor material tolerant to the combination of high temperatures, ammonia and potentially corrosive metal salts, as well as a long-term study on the cycle stability of the materials in the order of a few hundred to 1000 cycles. Last but not least, a detailed investigation of the volume-work of the materials on a larger scale is also necessary, as during reaction with NH_3 the material is expected to undergo significant expansion

Concluding the herein reported results we suggest, that transition metal ammoniates – and especially the reaction couple $CuSO_4$/ $[Cu(NH_3)_4]SO_4$ – should be considered for development of high-performance thermochemical energy storage processes, especially when merging small scales and high storage densities.

CRediT authorship contribution statement

Danny Müller: Conceptualization, Writing - original draft. **Christian Knoll:** Investigation. **Georg Gravogl:** Investigation. **Christian Jordan:** Data curation. **Elisabeth Eitenberger:** Investigation. **Gernot Friedbacher:** Resources. **Werner Artner:** Investigation. **Jan M. Welch:** Writing - review & editing. **Andreas Werner:** Project administration. **Michael Harasek:** Funding acquisition, Supervision. **Ronald Miletich:** Funding acquisition, Supervision. **Peter Weinberger:** Funding acquisition, Supervision.

Declaration of Competing Interest

The authors declare that they have no known competing financial interests or personal relationships that could have appeared to influence the work reported in this paper.

Acknowledgement

This work was financially supported by the Austrian Research Promotion Agency (FFG Forschungsförderungsgesellschaft), projects 853593, 841150 and 848876.

Appendix A. Supplementary material

Supplementary data to this article can be found online at https://doi.org/10.1016/j.apenergy.2021.116470.

References

[1] Farid MM, Khudhair AM, Razack SAK, Al-Hallaj S. A review on phase change energy storage: materials and applications. Energy Convers Manage 2004;45:1597–615.
[2] Kato Y. Thermal energy storage for sustainable energy consumption. Netherlands: Springer; 2007. p. 377–91.
[3] Ibrahim H, Ilinca A, Perron J. Energy storage systems—characteristics and comparisons. Renew Sustain Energy Rev 2008;12:1221–50.
[4] Jiang Z, Ji C, Qin H, Feng Z. Multi-stage progressive optimality algorithm and its application in energy storage operation chart optimization of cascade reservoirs. Energy. 2018;148:309–23.
[5] Jiang Z, Li R, Li A, Ji C. Runoff forecast uncertainty considered load adjustment model of cascade hydropower stations and its application. Energy. 2018;158:693–708.
[6] Kishore R, Priya S. A review on low-grade thermal energy harvesting: materials, methods and devices. Materials 2018;11:1433.
[7] Deepak K, Varma VB, Prasanna G, Ramanujan RV. Hybrid thermomagnetic oscillator for cooling and direct waste heat conversion to electricity. Appl Energy 2019;233–234:312–20.
[8] Thirugnanasambandam M, Iniyan S, Goic R. A review of solar thermal technologies☆. Renew Sustain Energy Rev 2010;14:312–22.
[9] Cabeza LFE. Advances in thermal energy storage systems - methods and applications. Elsevier; 2015.
[10] Agyenim F, Hewitt N, Eames P, Smyth M. A review of materials, heat transfer and phase change problem formulation for latent heat thermal energy storage systems (LHTESS). Renew Sustain Energy Rev 2010;14:615–28.
[11] Abedin AH, Rosen MR. A critical review of thermochemical energy storage systems. Open Renewable Energy J 2011;4:42–6.
[12] Hasnain SM. Review on sustainable thermal energy storage technologies, Part I: heat storage materials and techniques. Energy Convers Manage 1998;39:1127–38.

[13] Shukla A, Buddhi D, Sawhney RL. Solar water heaters with phase change material thermal energy storage medium: a review. Renew Sustain Energy Rev 2009;13:2119–25.
[14] Xu B, Li P, Chan C. Application of phase change materials for thermal energy storage in concentrated solar thermal power plants: a review to recent developments. Appl Energy 2015;160:286–307.
[15] Zalba B, Marín JM, Cabeza LF, Mehling H. Review on thermal energy storage with phase change: materials, heat transfer analysis and applications. Appl Thermal Eng 2003;23:251–83.
[16] Agrafiotis C, Becker A, Roeb M, Sattler C. Exploitation of thermochemical cycles based on solid oxide redox systems for thermochemical storage of solar heat. Part 5: Testing of porous ceramic honeycomb and foam cascades based on cobalt and manganese oxides for hybrid sensible/thermochemical heat storage. Sol Energy 2016;139:676–94.
[17] Alkilani MM, Sopian K, Alghoul MA, Sohif M, Ruslan MH. Review of solar air collectors with thermal storage units. Renew Sustain Energy Rev 2011;15:1476–90.
[18] Cabeza LF, Sole C, Castell A, Oro E, Gil A. Review of solar thermal storage techniques and associated heat transfer technologies. Proc IEEE 2012;100:525–38.
[19] Chidambaram LA, Ramana AS, Kamaraj G, Velraj R. Review of solar cooling methods and thermal storage options. Renew Sustain Energy Rev 2011;15:3220–8.
[20] Liu M, Saman W, Bruno F. Review on storage materials and thermal performance enhancement techniques for high temperature phase change thermal storage systems. Renew Sustain Energy Rev 2012;16:2118–32.
[21] N'Tsoukpoe KE, Liu H, Le Pierrès N, Luo L. A review on long-term sorption solar energy storage. Renew Sustain Energy Rev 2009;13:2385–96.
[22] Cot-Gores J, Castell A, Cabeza LF. Thermochemical energy storage and conversion: a-state-of-the-art review of the experimental research under practical conditions. Renew Sustain Energy Rev 2012;16:5207–24.
[23] Pinel P, Cruickshank CA, Beausoleil-Morrison I, Wills A. A review of available methods for seasonal storage of solar thermal energy in residential applications. Renew Sustain Energy Rev 2011;15:3341–59.
[24] Tian Y, Zhao CY. A review of solar collectors and thermal energy storage in solar thermal applications. Appl Energy 2013;104:538–53.
[25] Pardo P, Deydier A, Anxionnaz-Minvielle Z, Rougé S, Cabassud M, Cognet P. A review on high temperature thermochemical heat energy storage. Renew Sustain Energy Rev 2014;32:591–610.
[26] van Essen VM, Cot Gores J, Bleijendaal LPJ, Zondag HA, Schuitema R, Bakker M, et al. Characterization of salt hydrates for compact seasonal thermochemical storage. 2009:825–30.
[27] Yan J, Zhao CY. Experimental study of CaO/$Ca(OH)_2$ in a fixed-bed reactor for thermochemical heat storage. Appl Energy 2016;175:277–84.
[28] Gravogl G, Knoll C, Welch J, Artner W, Freiberger N, Nilica R, et al. Cycle stability and hydration behavior of magnesium oxide and its dependence on the precursor-related particle morphology. Nanomaterials. 2018;8:795.
[29] Müller D, Knoll C, Ruh T, Artner W, Welch JM, Peterlik H, et al. Calcium doping facilitates water dissociation in magnesium oxide. Adv Sustainable Syst 2018;2:1700096.
[30] Corgnale C, Hardy B, Motyka T, Zidan R. Metal hydride based thermal energy storage system requirements for high performance concentrating solar power plants. Int J Hydrogen Energy 2016;41:20217–30.
[31] Harries DN, Paskevicius M, Sheppard DA, Price TEC, Buckley CE. Concentrating solar thermal heat storage using metal hydrides. Proc IEEE 2012;100:539–49.
[32] André L, Abanades S, Flamant G. Screening of thermochemical systems based on solid-gas reversible reactions for high temperature solar thermal energy storage. Renew Sustain Energy Rev 2016;64:703–15.
[33] Block T, Schmücker M. Metal oxides for thermochemical energy storage: a comparison of several metal oxide systems. Sol Energy 2016;126:195–207.
[34] Müller D, Knoll C, Artner W, Harasek M, Gierl-Mayer C, Welch JM, et al. Combining in-situ X-ray diffraction with thermogravimetry and differential scanning calorimetry – An investigation of Co3O4, MnO2 and PbO2 for thermochemical energy storage. Sol Energy 2017;153:11–24.
[35] Kyaw K, Matsuda H, Hasatani M. Applicability of carbonation/decarbonation reactions to high-tempereture thermal energy storage and temperature upgrading. J Chem Eng Jpn 1996;29:119–25.
[36] Rhodes NR, Barde A, Randhir K, Li L, Hahn DW, Mei R, et al. Solar thermochemical energy storage through carbonation cycles of $SrCO_3$/SrO supported on $SrZrO_3$. ChemSusChem 2015;8:3793–8.
[37] Yamauchi K, Murayama N, Shibata J. Absorption and release of carbon dioxide with various metal oxides and hydroxides. Mater Trans 2007;48:2739–42.
[38] Fopah-Lele A, Tamba JG. A review on the use of SrBr 2 ·6_H2O as a potential material for low temperature energy storage systems and building applications. Sol Energy Mater Sol Cells 2017;164:175–87.
[39] Manickam K, Mistry P, Walker G, Grant D, Buckley CE, Humphries TD, et al. Future perspectives of thermal energy storage with metal hydrides. Int J Hydrogen Energy 2019;44:7738–45.
[40] Agrafiotis C, Roeb M, Schmücker M, Sattler C. Exploitation of thermochemical cycles based on solid oxide redox systems for thermochemical storage of solar heat. Part 1: Testing of cobalt oxide-based powders. Sol Energy 2014;102:189–211.
[41] Alonso E, Hutter C, Romero M, Steinfeld A, Gonzalez-Aguilar J. Kinetics of Mn_2O_3–Mn_3O_4 and Mn_3O_4–MnO redox reactions performed under concentrated thermal radiative flux. Energy Fuels 2013;27:4884–90.
[42] Carrillo AJ, Sastre D, Serrano DP, Pizarro P, Coronado JM. Revisiting the BaO_2/BaO redox cycle for solar thermochemical energy storage. Phys Chem Chem Phys. 2016;18:8039–48.
[43] Ervin G. Solar heat storage using chemical reactions. J Solid State Chem 1977;22:51–61.
[44] Möller S, Palumbo R. The development of a solar chemical reactor for the direct thermal dissociation of zinc oxide. J Sol Energy Eng 2001;123:83.
[45] Neises M, Tescari S, de Oliveira L, Roeb M, Sattler C, Wong B. Solar-heated rotary kiln for thermochemical energy storage. Sol Energy 2012;86:3040–8.
[46] Kuravi S, Goswami Y, Stefanakos EK, Ram M, Jotshi C, Pendyala S, et al. Thermal energy storage for concentrating solar power plants. Technol Innov 2012;14:81–91.
[47] Gravogl G, Knoll C, Artner W, Welch JM, Eitenberger E, Friedbacher G, et al. Pressure effects on the carbonation of MeO (Me = Co, Mn, Pb, Zn) for thermochemical energy storage. Appl Energy 2019;252:113451.
[48] Dunn R, Lovegrove K, Burgess G. A review of ammonia-based thermochemical energy storage for concentrating solar power. Proc IEEE 2012;100:391–400.
[49] Liu C, Li F, Ma L-P, Cheng H-M. Advanced Materials for Energy Storage. Adv Mater 2010;22:E28–62.
[50] Luzzi A, Lovegrove K, Filippi E, Fricker H, Schmitz-goeb M, Chandapillai M, et al. Techno-economic analysis of a 10 MWe solar thermal power plant using ammonia-based thermochemical energy storage. Sol Energy 1999;66:91–101.
[51] Siddiq S, Khushnood S, Koreshi ZU, Shah MT, Qureshi AH. Optimal energy recovery from ammonia synthesis in a solar thermal power plant. Arabian J Sci Eng 2013;38:2569–77.
[52] Herrmann U, Kearney DW. Survey of thermal energy storage for parabolic trough power plants. J Sol Energy Eng 2002;124:145.
[53] Lavine AS, Lovegrove KM, Jordan J, Anleu GB, Chen C, Aryafar H, et al. Thermochemical energy storage with ammonia: aiming for the sunshot cost target. 2016;1734:050028.
[54] Lepinasse E, Spinner B. Production de froid par couplage de réacteurs solide-gaz I: analyse des performances de tels systèmes. Int J Refrig 1994;17:309–22.
[55] Lovegrove K, Kreetz H, Luzzi A. The first ammonia based solar thermochemical energy storage demonstration. Le. J Phys IV 1999;09. Pr3-581-Pr3-6.
[56] Lovegrove K, Luzzi A, Kreetz H. A solar-driven ammonia-based thermochemical energy storage system. Sol Energy 1999;67:309–16.
[57] Lovegrove K, Luzzi A, Soldiani I, Kreetz H. Developing ammonia based thermochemical energy storage for dish power plants. Sol Energy 2004;76:331–7.
[58] Deutsch M, Müller D, Aumeyr C, Jordan C, Gierl-Mayer C, Weinberger P, et al. Systematic search algorithm for potential thermochemical energy storage systems. Appl Energy 2016;183:113–20.
[59] Dunlap RM. Thermochemical energy storage and mechanical energy converter system. Google Patents; 1982.
[60] Aidoun Z, Ternan M. Pseudo-stable transitions and instability in chemical heat pumps: the NH_3–$CoCl_2$ system. Appl Therm Eng 2001;21:1019–34.
[61] Trudel J, Hosatte S, Ternan M. Solid–gas equilibrium in chemical heat pumps: the NH_3–$CoCl_2$ system. Appl Therm Eng 1999;19:495–511.
[62] Jiang L, Zhu FQ, Wang LW, Liu CZ, Wang RZ. Experimental investigation on a $MnCl_2$ –$CaCl_2$ –NH_3 thermal energy storage system. Renewable Energy 2016;91:130–6.
[63] van der Pal M, Critoph RE. Performance of $CaCl_2$-reactor for application in ammonia-salt based thermal transformers. Appl Therm Eng 2017;126:518–24.
[64] Sharonov VE, Veselovskaya JV, Aristov YI. Ammonia sorption on composites 'CaCl$_2$ in inorganic host matrix': isosteric chart and its performance. Int J Low-Carbon Technol 2006;1:191–200.
[65] Al-Zareer M, Dincer I, Rosen MA. Heat transfer and thermodynamic analyses of a novel solid-gas thermochemical strontium chloride-ammonia thermal energy storage system. J Heat Transfer 2017;140:022802.
[66] Liu CY, Aika K-i. Ammonia absorption on alkaline earth halides as ammonia separation and storage procedure. Bull Chem Soc Jpn 2004;77:123–31.
[67] Elmøe TD, Sørensen RZ, Quaade U, Christensen CH, Nørskov JK, Johannessen T. A high-density ammonia storage/delivery system based on $Mg(NH_3)_6Cl_2$ for SCR–DeNO$_x$ in vehicles. Chem Eng Sci 2006;61:2618–25.
[68] Johannessen T, Christensen CH, Norskov JK, Quaade U, Sorensen RZ. High density storage of ammonia. US 2009/0123361 A1; 2009.
[69] Breternitz J, Vilk YE, Giraud E, Reardon H, Hoang TKA, Godula-Jopek A, et al. Facile uptake and release of ammonia by nickel halide ammines. ChemSusChem 2016;9:1312–21.
[70] Han JH, Lee K-H, Kim DH, Kim H. Transformation analysis of thermochemical reactor based on thermophysical properties of graphite−MnCl2 complex. Ind Eng Chem Res 2000;39:4127–39.
[71] Sharma R, Anil Kumar E. Study of ammoniated salts based thermochemical energy storage system with heat up-gradation: a thermodynamic approach. Energy. 2017;141:1705–16.
[72] Michel B, Mazet N, Neveu P. Experimental investigation of an innovative thermochemical process operating with a hydrate salt and moist air for thermal storage of solar energy: Global performance. Appl Energy 2014;129:177–86.
[73] (Editor-in-Chief) MS. Comprehensive Handbook of Calorimetry and Thermal Analysis. Japan Society of Calorimetry and Thermal Analysis (Editor), Wiley. 2004:556.
[74] Huheey JE, Keiter EA, Keiter RL, Medhi OK. Inorganic chemistry: principles of structure and reactivity. 4th ed. Pearson Education; 2006.
[75] Unfallversicherung DG. GESTIS-Stoffdatenbank. http://gestisitrustde/nxt/gatewaydll/gestis_de/000000xml?f=templates&fn=defaulthtm&vid=gestisdeu:sdbdeu; 2020.
[76] Nilsson KB, Eriksson L, Kessler VG, Persson I. The coordination chemistry of the copper(II), zinc(II) and cadmium(II) ions in liquid and aqueous ammonia solution, and the crystal structures of hexaamminecopper(II) perchlorate and chloride, and hexaamminecadmium(II)chloride. J Mol Liq 2007;131–132:113–20.

[77] Wagmann D, Evans W, Parker V, Schumm R, Halow I, Bailey S, et al. The NBS tables of chemical thermodynamic properties. J Phys Chem Ref Data 1982;11.
[78] Rejitha KS, Ichikawa T, Mathew S. Thermal decomposition studies of $[Ni(NH_3)_6]X_2$ (X = Cl, Br) in the solid state using TG-MS and TR-XRD. J Therm Anal Calorim 2010;103:515–23.
[79] Airò Farulla G, Cellura M, Guarino F, Ferraro M. A review of thermochemical energy storage systems for power grid support. Appl Sci 2020;10:3142.
[80] Malley-Ernewein A, Lorente S. Analysis of thermochemical energy storage in an elemental configuration. Sci Rep 2019;9.